

**Anderson localization and Brewster anomalies in photonic disordered quasiperiodic lattices**E. Reyes-Gómez,<sup>1</sup> A. Bruno-Alfonso,<sup>2</sup> S. B. Cavalcanti,<sup>3</sup> and L. E. Oliveira<sup>4</sup><sup>1</sup>*Instituto de Física, Universidad de Antioquia, AA 1226, Medellín, Colombia*<sup>2</sup>*Faculdade de Ciências, UNESP-Universidade Estadual Paulista, 17033-360 Bauru-SP, Brazil*<sup>3</sup>*Instituto de Física, Universidade Federal de Alagoas, 57072-970 Maceió-AL, Brazil*<sup>4</sup>*Instituto de Física, Universidade Estadual de Campinas-UNICAMP, 13083-859 Campinas-SP, Brazil*

(Received 26 April 2011; revised manuscript received 28 August 2011; published 21 September 2011)

A comprehensive study of the properties of light propagation through one-dimensional photonic disordered quasiperiodic superlattices, composed of alternating layers with random thicknesses of air and a dispersive metamaterial, is theoretically performed. The superlattices consist of the successive stacking of  $N$  quasiperiodic Fibonacci or Thue-Morse heterostructures. The width of the slabs in the photonic superlattice may randomly fluctuate around its mean value, which introduces a structural disorder into the system. It is assumed that the left-handed layers have a Drude-type dispersive response for both the dielectric permittivity and magnetic permeability, and Maxwell's equations are solved for oblique incidence by using the transfer-matrix formalism. The influence of both quasiperiodicity and structural disorder on the localization length and Brewster anomalies are thoroughly discussed.

DOI: [10.1103/PhysRevE.84.036604](https://doi.org/10.1103/PhysRevE.84.036604)

PACS number(s): 41.90.+e, 42.25.Dd, 72.15.Rn, 78.67.Pt

**I. INTRODUCTION**

Wave propagation through layered media has been investigated since Lord Rayleigh's studies, by the end of the XIX century, on laminated one-dimensional (1D) structures [1]. Recently, photonic crystals, metamaterials, and plasmonics have given a new thrust to investigations on light propagation through heterostructures, due to the engineering of artificial optical materials. A typical example is a left-handed material (LHM) that exhibits negative refraction [2]. In a LHM, the phase velocity of light points to the opposite direction relative to the flow of energy in contrast with a right-handed material (RHM). LHMs have opened up new exciting possibilities in light manipulation, such as cloaking and super lenses. These LHMs also display optical magnetism in the sense that the magnetic component of the optical field plays an active role in its interaction with light. Optical magnetism has been exhibited by 1D superlattices composed of the repetition of an elementary cell consisting of a RHM-LHM double-layer (henceforth referred to as meta-stacks), bringing up features of light-matter interaction with no counterpart in RHM-RHM superlattices. To cite a few, electric- and magnetic-plasmon polaritons [3,4], Brewster angles in a transversal electric (TE) configuration [5] and suppression of Anderson localization in disordered periodic chains [6–8].

As a natural extension, investigations on superlattices that alternate a RHM and a LHM according to a Fibonacci structure have demonstrated that the robust  $\langle n \rangle = 0$ -gap, known to exist in its periodic counterpart, is also present in the Fibonacci metastack. In a periodic chain, the frequency that characterizes the  $\langle n \rangle = 0$ -gap is obtained by choosing a unit ratio between the optical paths of alternate layers. One should note here that, in a periodic system, for equal optical paths the phase acquired in the RHM layer is exactly balanced, in average, by the phase lost in the LHM layer. Therefore, there is no light propagation. This balance in a Fibonacci metastack is achieved by choosing the golden ratio as the ratio of the optical paths of alternate layers [9]. Also, a photonic Cantor-like frequency spectrum is obtained in Fibonacci or Thue-Morse

metastacks [10,11]. Studies on both periodic and quasiperiodic metastacks have revealed further unexpected properties such as the existence of longitudinal plasmon-polariton excitations under the oblique incidence of light, due to the existence of electric and/or magnetic field components along the stacking direction. These plasmon polaritons are of electric nature in a transversal magnetic (TM) incidence configuration and of magnetic nature in a TE configuration.

A further practical consideration one should be concerned with in superlattices containing a LHM element is that LHMs are engineered from metal-dielectric structures, and the disorder-induced losses in such systems may be of considerable importance, especially in the visible range [12]. The influence of disorder on the properties of light propagation in photonic crystals has been a subject of a considerable amount of work in the last few years. Disorder affects a wide variety of its physical properties, causes multiple light scattering, originates the extinction of coherent waves propagating through the photonic structure, and leads to a dramatic change of the localization properties of the electromagnetic modes. In this sense, the Anderson localization of light in disordered photonic crystals has been widely studied both from the experimental and theoretical points of view [6–8,13–23]. Considering the richness found in quasiperiodic RHM superlattices as compared to the periodic case, the aim of the present work is to theoretically investigate the light-localization properties in disordered Fibonacci and Thue-Morse photonic metastacks as well as the influence of both the structural disorder and quasiperiodicity on the Anderson localization length. The paper is organized as follows. Section II is devoted to explain the theoretical basis of the calculations, as well as to characterize the Fibonacci and Thue-Morse heterostructures. Numerical results and discussion are presented in Sec. III, and final conclusions are given in Sec. IV.

**II. THEORETICAL FRAMEWORK**

Let us turn our attention to a finite 1D photonic superlattice consisting of the successive stacking, along the  $z$  direction,

of  $N$  quasiperiodic Fibonacci or Thue-Morse heterostructures of order  $j$ , labeled as  $S_j$ , which play the role of unit cells of the finite superlattice [11]. Each superlattice is considered to be composed by a pair of optical materials  $A$  and  $B$ , whose electric permittivities and magnetic permeabilities are given by  $\epsilon_A = \mu_A = 1$  (air) and Drude-like metamaterial dispersion responses as [24]  $\epsilon_B(\omega) = \epsilon_0 - \frac{\omega_p^2}{\omega^2}$  and  $\mu_B(\omega) = \mu_0 - \frac{\omega_m^2}{\omega^2}$ . The frequencies associated with the electric and magnetic plasmon modes are, therefore,  $\nu_e = \omega_e/(2\pi\sqrt{\epsilon_0})$  and  $\nu_m = \omega_m/(2\pi\sqrt{\mu_0})$ , respectively.

The quasiperiodic unit cell of the superlattice is of either the Fibonacci or Thue-Morse type. In both cases, all unit cells  $S_j$  are of the same quasiperiodic type and same order  $j$ . On the one hand, the  $j$ th Fibonacci unit cell  $S_j$  may be obtained by the recursive concatenation rule  $S_j(A, B) = S_{j-1}(A, B)S_{j-2}(A, B)$  and the initial conditions  $S_0(A, B) = B$  and  $S_1(A, B) = A$ . The total number of elements ( $A$  and  $B$ ) in  $S_j$  is  $C_j$ , satisfying  $C_j = C_{j-1} + C_{j-2}$  and  $C_0 = C_1 = 1$ . Moreover, the number of layers  $A$  ( $B$ ) is  $C_j^A = C_{j-1}$  ( $C_j^B = C_{j-2}$ ). On the other hand, the  $j$ th Thue-Morse unit cell  $S_j$  satisfy  $S_j(A, B) = S_{j-1}(A, B)S_{j-1}(B, A)$  and  $S_1(A, B) = AB$ . In this case,  $C_j = 2^j$  and  $C_j^A = C_j^B = 2^{j-1}$ .

Once the sequence of  $N C_j$  layers in the superlattice has been obtained, disorder is introduced by randomly choosing the width of each layer. If the  $k$ th layer is made of material  $A$  ( $B$ ), then its thickness  $a_k$  ( $b_k$ ) is treated as a random variable with uniform distribution over the interval  $[a - \Delta/2, a + \Delta/2]$  ( $[b - \Delta/2, b + \Delta/2]$ ). The parameter  $\Delta$  is called the disorder amplitude. Of course, it is positive and less than the smallest length between  $a$  and  $b$ .

From the theoretical point of view, many geometrical and physical properties of the disordered system are usually determined by averaging over a sufficiently large ensemble of superlattices. Each element of the ensemble is called as a realization of the superlattice and is generated by following the procedure described above. For any geometrical or physical magnitude  $\mathcal{P}$  associated to the superlattice, the experimental value is estimated by the average  $\langle \mathcal{P} \rangle$  over the considered ensemble. For instance, the averaged length is  $\langle L \rangle = N(C_j^A a + C_j^B b)$ . Of course,  $a$  and  $b$  correspond to the average width of the slabs  $A$  and  $B$ , respectively.

For each realization of the superlattice, one may calculate the light-transmission coefficient. This is the ratio between the intensities of an incident beam and the resulting transmitted beam. By choosing the  $z$  axis along the stacking direction and the origin of coordinates at the left interface, we obtain the dielectric permittivity  $\epsilon(z)$ , the magnetic permeability  $\mu(z)$ , and the refractive index  $n(z) = \sqrt{\mu(z)}\sqrt{\epsilon(z)}$ . Therefore, the electric-field amplitude  $E(z)$  of a monochromatic and transversal electric (TE) wave propagating through the superlattice satisfy the following differential equation

$$\frac{d}{dz} \left[ \frac{1}{\mu(z)} \frac{d}{dz} E(z) \right] = -\epsilon(z) \left[ \frac{\omega^2}{c^2} - \frac{q^2}{n^2(z)} \right] E(z), \quad (1)$$

where  $\omega$  is the angular frequency,  $q = \frac{\omega}{c} n_A \sin(\theta)$  is the component of the wave vector parallel to the interfaces and  $\theta$  is the incidence angle in the medium  $A$ . A similar equation applies for the transversal magnetic (TM) waves and may be obtained from Eq. (1) by permuting  $\mu(z)$  and  $\epsilon(z)$  and by

replacing  $E(z)$  by  $H(z)$ . In the present work, we restrict the attention to TE modes.

The calculation of the transmission coefficient is performed by following the transfer-matrix procedure [11]. The transmission coefficient of TE waves is given by  $T = |t|^2$ , where  $t$  satisfies

$$\frac{2}{t} = (1, -i\mu_A/Q_A) \mathbb{M}^{-1} \begin{pmatrix} 1 \\ iQ_A/\mu_A \end{pmatrix}, \quad (2)$$

with  $Q_A = \frac{\omega}{c} n_A \cos(\theta)$  and  $\mathbb{M}$  being the transfer matrix given in Ref. [11]. Once the transmission coefficient is found for each superlattice of the ensemble, one may obtain the quantity

$$\xi_N = - \left\langle \frac{\ln(T)}{2L} \right\rangle^{-1}, \quad (3)$$

and the localization length  $\xi$  is given by [16,25]

$$\xi = \lim_{N \rightarrow \infty} \xi_N. \quad (4)$$

Here the limit  $N \rightarrow \infty$  is understood as  $L \rightarrow \infty$ .

### III. RESULTS AND DISCUSSION

The behavior of  $\xi_N$  associated with the TE electromagnetic modes, as a function of the number  $N$  of Fibonacci sequences  $S_j$  ( $j = 2, 3, 4, 5$ ) in the photonic superlattice, is displayed in Fig. 1. Numerical results were obtained for  $\nu = 5$  THz,

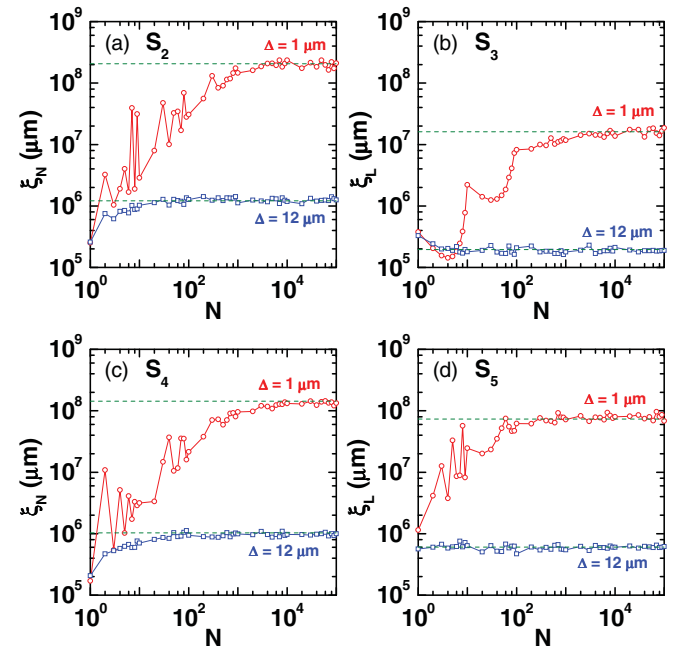


FIG. 1. (Color online)  $\xi_N$  [cf. Eq. (3)], corresponding to the TE modes, as a function of the number  $N$  of Fibonacci sequences  $S_j$  contained in the photonic heterostructure. Results displayed in (a), (b), (c), and (d) were computed for  $j = 2$ ,  $j = 3$ ,  $j = 4$ , and  $j = 5$ , respectively. In each panel, calculations were performed for  $\nu = 5$  THz,  $\theta = \pi/6$ ,  $\epsilon_0 = 1.21$ ,  $\mu_0 = 1$ ,  $\omega_e = \omega_m = 6\pi$  THz,  $a = b = 12 \mu\text{m}$ , 100 realizations of disorder, and for two different values of the disorder amplitude  $\Delta$ . Horizontal dashed lines correspond to the respective localization lengths, i.e., to the limit of  $\xi_N$  for sufficiently large values of  $N$  [cf. Eq. (4)].

$\theta = \pi/6$ ,  $\epsilon_0 = 1.21$ ,  $\mu_0 = 1$ ,  $\omega_e = \omega_m = 6\pi$  THz,  $a = b = 12 \mu\text{m}$ , and 100 realizations of disorder. Circles and squares correspond to  $\Delta = 1 \mu\text{m}$  and  $\Delta = 12 \mu\text{m}$ , respectively. For low and moderate values of the system size, the magnitude  $\xi_N$  presents a strong dependence on the number  $N$  of unit cells. However, beyond a certain value of  $N$ ,  $\xi_N$  slightly oscillates around its limiting value (cf. horizontal dashed lines in Fig. 1). One may expect that, in the limit  $N \rightarrow \infty$ ,  $\xi_N$  leads to the localization length within the accuracy of the numerical calculation. We have verified that such limiting value does not sensitively depend on the number of realizations (results not shown here). In that way, one is able to find a practical criterium to obtain the optima values for both the system length and the number of realizations in order to compute the localization length.

The localization length in units of the averaged system length is displayed in Fig. 2 as a function of the wave frequency. Numerical results were obtained for four different photonic heterostructures, each consisting of the corresponding stacking of a  $S_j$  Fibonacci sequence. One may note from Fig. 2 the existence of different values of the wave frequency at which the localization length increases several orders of magnitude beyond the averaged system length. This fact is due to the Brewster phenomenon. It is well known that for a given

electromagnetic wave, monochromatic and TE-polarized, which is incident on a nonabsorptive medium, there exists a value of the incident angle at which the reflected wave is fully suppressed. Equivalently, if the TE and monochromatic electromagnetic wave arrives at the medium with a given incidence angle, one may find a set of frequency values at which the reflected wave is suppressed. The Brewster phenomenon, which takes place also in disordered systems, leads to a transmission coefficient equal to one and, therefore, to an infinite localization length. In disordered systems, the boost of the localization length at the Brewster angle is known as Brewster anomaly. It has been shown [7,8] that, in weakly disordered 1D systems, the frequency  $\omega_0$  and the angle  $\theta_0$  at which the Brewster anomaly occurs are related by the general expression

$$\frac{f_A(\omega_0, \theta_0)}{f_B(\omega_0, \theta_0)} = \frac{f_B(\omega_0, \theta_0)}{f_A(\omega_0, \theta_0)}, \quad (5)$$

where

$$f_x^{\text{TE}}(\omega, \theta) = \frac{\sqrt{\epsilon_x(\omega)\mu_x(\omega) - n_A^2 \sin^2(\theta)}}{\mu_x(\omega)} \quad (6)$$

for the TE modes,

$$f_x^{\text{TM}}(\omega, \theta) = \frac{\sqrt{\epsilon_x(\omega)\mu_x(\omega) - n_A^2 \sin^2(\theta)}}{\epsilon_x(\omega)} \quad (7)$$

for the TM modes, and  $x$  is equal to  $A$  or  $B$ . The frequency values  $\nu_0 = \omega_0/2\pi$  predicted by Eq. (5) at which the Brewster anomalies take place for  $\theta_0 = \pi/6$  have been displayed in all panels of Fig. 2 as vertical dashed lines. It is apparent from Fig. 2 that the predicted values of  $\nu_0$  perfectly match the present numerical calculations for the positions of the Brewster anomalies in the frequency spectrum. Although Eq. (5) was obtained for weakly disordered systems, it seems to be quite general because it also applies for periodic photonic systems with intermediate or large values of disorder amplitude [8], as well as for disordered quasiperiodic superlattices. Even though the localization length may be dramatically modified by changing the parameter  $\Delta$  or the Fibonacci sequence in the elementary cell, the positions of the Brewster anomalies in the frequency spectrum remain unchanged.

For the sake of investigating the general character of Eq. (5), we have calculated the TE localization length in several disordered Fibonacci photonic crystals for different values of the ratio  $b/a$ . Numerical results for  $b/a = 2$  are shown in Fig. 3. In addition, Fig. 4 displays the numerical results for the TE localization length in quasiperiodic Thue-Morse heterostructures. As in Fig. 2, calculations in both Figs. 3 and 4 were performed for an incidence angle  $\theta = \pi/6$ . In all cases, the calculated positions of the Brewster anomalies in the frequency spectra coincide with those predicted by Eq. (5). The above-discussed results indicate that, in 1D disordered systems, the positions of the Brewster anomalies in the frequency spectra do not depend on the degree of disorder, or on the average length of the individual layers, or on the kind of structure of the elementary cell (periodic or quasiperiodic).

Now we study the asymptotical behavior of the localization length in the limit of low and high frequencies. By following previous works [6,7], we have calculated the localization

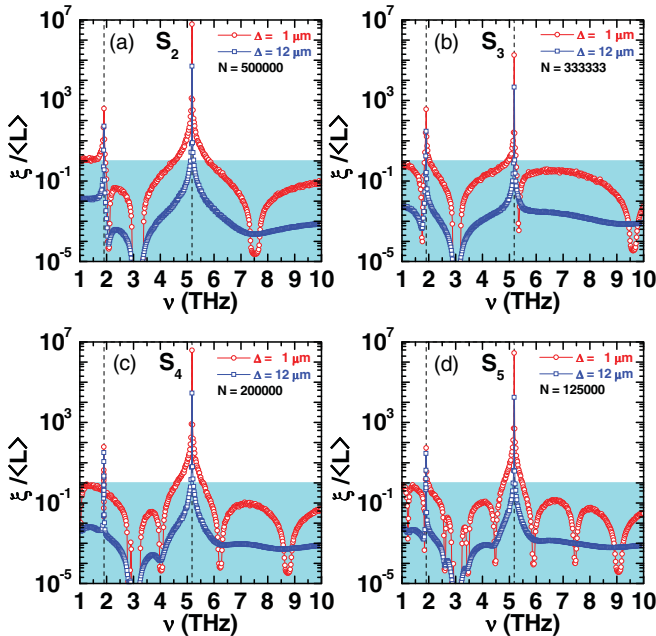


FIG. 2. (Color online) TE localization length in units of the averaged system length  $\langle L \rangle$ , as a function of the electromagnetic-wave frequency, for four different photonic heterostructures, each consisting of the corresponding stacking of a  $S_j$  Fibonacci sequence. The number of sequences  $N$  used in each panel was chosen in order to approximately guarantee the same value of  $\langle L \rangle$  for each value of  $j$ . Numerical results were obtained for  $\theta = \pi/6$ ,  $\epsilon_0 = 1.21$ ,  $\mu_0 = 1$ ,  $\omega_e = \omega_m = 6\pi$  THz,  $a = b = 12 \mu\text{m}$ , and for 100 realizations of disorder. Circles and squares correspond to  $\Delta = 1 \mu\text{m}$  and  $\Delta = 12 \mu\text{m}$ , respectively. Vertical dashed lines correspond to the frequencies  $\nu_0 = \omega_0/2\pi$  predicted by Eq. (5) for  $\theta_0 = \pi/6$ . Shadow areas correspond to the regions ( $\xi/\langle L \rangle < 1$ ) in which the TE modes are localized.

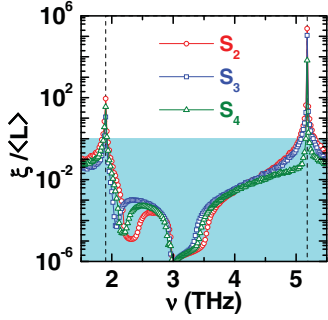


FIG. 3. (Color online) Frequency-dependent TE localization length, in units of the averaged system length, corresponding to three different photonic heterostructures, each consisting of the corresponding stacking of a  $S_j$  Fibonacci sequence. Circles, squares, and triangles correspond to  $S_2$ ,  $S_3$ , and  $S_4$  Fibonacci sequences, respectively. Numerical results were obtained for  $\theta = \pi/6$ ,  $\epsilon_0 = 1.21$ ,  $\mu_0 = 1$ ,  $\omega_e = \omega_m = 6\pi$  THz,  $a = 6 \mu\text{m}$ ,  $b = 12 \mu\text{m}$ ,  $\Delta = 6 \mu\text{m}$ , and for 100 realizations of disorder. We have used  $N = 666667$  for  $S_2$ ,  $N = 500000$  for  $S_3$ , and  $N = 285714$  for  $S_4$  in order to approximately obtain the same value of  $\langle L \rangle$  in each case. Shadow areas correspond to the regions ( $\xi/\langle L \rangle < 1$ ) in which the TE modes are localized.

length for TE modes as a function of the vacuum wavelength  $\lambda = 2\pi c/\omega$ . Results are displayed in Fig. 5 for four different photonic heterostructures, each consisting of the corresponding stacking of a  $S_j$  Fibonacci sequence. In each case, the number  $N$  of the Fibonacci sequences stacked in the finite system was chosen in order to approximately guarantee the same value of the averaged system length  $\langle L \rangle$  for each value of the Fibonacci order  $j$ . Numerical results were obtained for normal incidence and using the same set of parameters as in Fig. 1. One may distinguish three different regimes in the behavior of  $\xi/\langle L \rangle$ . First, in the short-wavelength regime ( $\lambda < 1 \mu\text{m}$ ), the localization length does not depend (or weakly depends) on  $\lambda$ . For intermediate values of  $\lambda$  ( $1 \mu\text{m} < \lambda < 10^3 \mu\text{m}$ ),

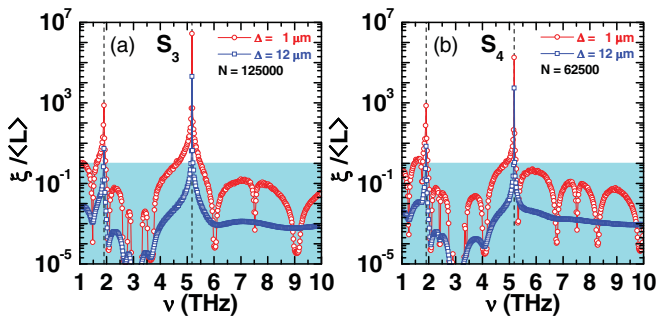


FIG. 4. (Color online) Frequency dependence of the TE localization length, in units of the averaged system length  $\langle L \rangle$ , for two different photonic heterostructures, each consisting of the corresponding stacking of a different Thue-Morse sequence,  $S_3$  or  $S_4$ . The number of sequences  $N$  used in each panel was chosen in order to obtain the same value of  $\langle L \rangle$  used in Fig. 2. Numerical results were obtained for  $\theta = \pi/6$ ,  $\epsilon_0 = 1.21$ ,  $\mu_0 = 1$ ,  $\omega_e = \omega_m = 6\pi$  THz,  $a = b = 12 \mu\text{m}$ , and for 100 realizations of disorder. Circles and squares correspond to  $\Delta = 1 \mu\text{m}$  and  $\Delta = 12 \mu\text{m}$ , respectively, whereas shadow areas correspond to the regions ( $\xi/\langle L \rangle < 1$ ) in which the TE modes are localized.

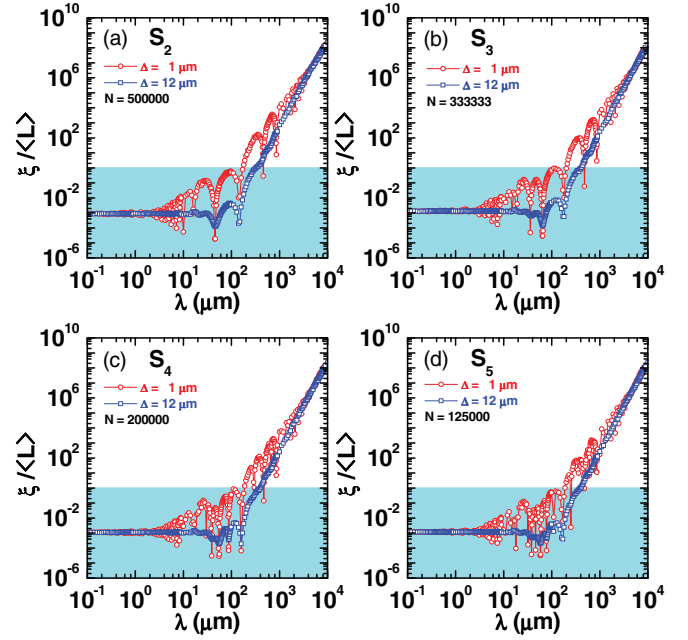


FIG. 5. (Color online) Localization length (TE modes) in units of the average system length  $\langle L \rangle$ , as a function of the vacuum wavelength  $\lambda = 2\pi c/\omega$ , for four different photonic heterostructures, each consisting of the corresponding stacking of a  $S_j$  Fibonacci sequence. The number of sequences  $N$  used in each panel was chosen in order to approximately guarantee the same value of  $\langle L \rangle$  for each value of  $j$ . Numerical results were obtained for normal incidence,  $\epsilon_0 = 1.21$ ,  $\mu_0 = 1$ ,  $\omega_e = \omega_m = 6\pi$  THz,  $a = b = 12 \mu\text{m}$ , and for 100 realizations of disorder. Circles and squares correspond to  $\Delta = 1 \mu\text{m}$  and  $\Delta = 12 \mu\text{m}$ , respectively. Shadow areas correspond to the regions ( $\xi/\langle L \rangle < 1$ ) in which the TE modes are localized.

the localization length, in units of the averaged system length, displays an oscillatory behavior. Finally, in the long-wavelength regime the localization length in units of  $\langle L \rangle$  increases as a power of  $\lambda$ . In the intermediate wavelength regime and for low levels of disorder, the effects of the quasiperiodicity result in an increasing on the oscillatory behavior of the localization length as the Fibonacci order  $j$  is increased. The oscillations of the localization length as a function of the wavelength are related with the presence of frequency regions at which the transmission coefficient falls. Such frequency regions actually behave as pseudogaps in the finite weakly disordered heterostructure. It is well known that the number of pseudogaps in the frequency spectrum of a Fibonacci photonic crystal increases as the Fibonacci order of the elementary cell is increased, a fact which is a consequence of the change of the long-range spatial coherence of the electromagnetic modes due to the quasiperiodicity. Therefore, an increasing of the quasiperiodic order of the elementary cell leads to an increasing of the oscillations of  $\xi$  as a function of  $\lambda$ . One also may note that the amplitude of such oscillations decreases as the parameter  $\Delta$ , which controls the magnitude of the structural disorder, is increased. The decay of the amplitudes of the above-described oscillations as  $\Delta$  increases is the result of an increasing of the destructive interferences of the electromagnetic waves which are multiply scattered inside the system, a physical situation

in which the pseudogap structure of the frequency spectrum disappears.

Present numerical calculations of the localization length as a function of the wavelength for disordered quasiperiodic photonic superlattices qualitatively agree with previous theoretical results reported by Asatryan *et al.* [6] for normal incidence and disordered (in the refraction indices) systems. Numerical results displayed in Fig. 5 may be fitted by the simple expressions

$$\frac{\xi}{\langle L \rangle} = \alpha \quad (8)$$

and

$$\frac{\xi}{\langle L \rangle} = \left( \frac{\lambda}{\beta} \right)^\gamma \quad (9)$$

in the short- Eq. (8) and long-wavelength Eq. (9) regimes, respectively. In the above expressions  $\alpha$ ,  $\beta$ , and  $\gamma$  are coefficients determining the asymptotic behavior of  $\xi$ . The coefficient  $\alpha$  represents the localization length, in units of the system length, in the short wavelength limit. The characteristic wavelength  $\beta$  means the wavelength value at which the electromagnetic modes become delocalized. Moreover, the coefficient  $\gamma$  governs the power law describing the asymptotical behavior of the localization length in the long wavelength limit. We have performed a statistical analysis of the numerical data displayed in Fig. 5. The coefficients  $\alpha$ ,  $\beta$ , and  $\gamma$  are then shown in Fig. 6 as functions of the Fibonacci order  $j$  of the elementary cell. Statistical errors have also been included as error bars. Apart from the random structural disorder imposed to the system, quasiperiodicity can also cause multiple scattering of electromagnetic waves that lead to the extinction of coherent waves propagating in the photonic heterostructure. This physical situation is manifested in a dependence of coefficients  $\alpha$ ,  $\beta$ , and  $\gamma$  with the order  $j$  of the unit cell. One may note from Fig. 6 that quasiperiodicity slightly affects the behavior of  $\xi/\langle L \rangle$  in the short wavelength limit. In the long wavelength limit, however, the effects of the quasiperiodicity on the localization length are more dramatic. In addition, in all cases studied here, the coefficient  $\gamma$  slightly differs from the value  $\gamma = 6$  predicted by Asatryan *et al.* [6].

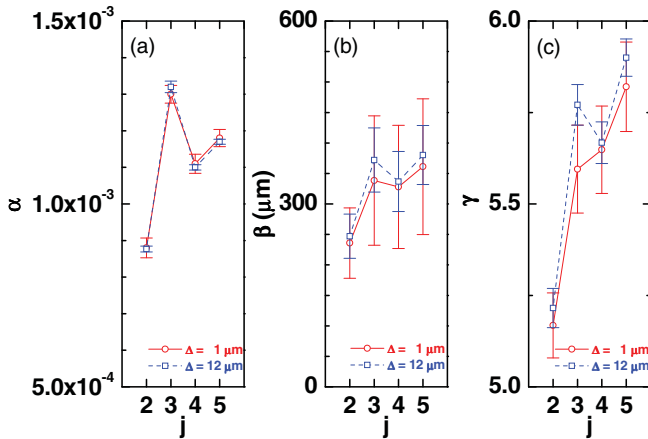


FIG. 6. (Color online) Parameters  $\alpha$ ,  $\beta$ , and  $\gamma$  [cf. Eqs. (8) and (9)]. Results were obtained from a statistical analysis of the numerical results displayed in Fig. 5.

We would like to stress that the localization length is determined, in part, by the frequency dependence of the magnetic permeabilities and dielectric susceptibilities corresponding to the optical materials composing the photonic superlattice. This may be of particular importance in the low-frequency limit, where the above obtained asymptotic behavior of the localization length could be affected if different dielectric and magnetic responses are chosen. In particular, long wavelength results obtained in Fig. 5 are not reliable due to the divergence of  $\mu_B$  as  $\omega \rightarrow 0$  in the Drude-like frequency dependence of the magnetic permeability. In order to further investigate the behavior of the localization length in the limit  $\lambda \rightarrow \infty$ , it is then advisable to consider magnetic susceptibilities corresponding to real physical systems in slabs  $B$ . As it is well known, for split-ring resonator metamaterials, the dielectric permittivity may be taken as in the Drude model, whereas the magnetic permeability may be written as [26–28]

$$\mu_B(\omega) = \mu_0 - \frac{F\omega^2}{\omega^2 - \omega_m^2 + i\gamma_m\omega}, \quad (10)$$

where  $\gamma_m$  is the magnetic damping constant, and  $F < \mu_0$  is a positive parameter determined by the geometry of the split ring [27]. Here we have taken, for simplicity,  $\gamma_m = 0$ . In this case, the frequency associated with the magnetic plasmon mode is related with the resonance frequency  $\omega_m$  by the expression  $\nu_m = \omega_m \sqrt{\mu_0} / (2\pi \sqrt{\mu_0 - F})$ .

By using a more realistic magnetic response of the metamaterial slabs [cf. Eq. (10)], we have displayed in Fig. 7 the localization length in units of  $\langle L \rangle$  as a function of  $\lambda$  in four different Fibonacci unit cells. Calculations were performed for  $\epsilon_0 = 1.21$ ,  $\mu_0 = 1$ ,  $\omega_e = \omega_m = 6\pi$  THz,  $a = b = 12 \mu\text{m}$ ,  $F = 0.25$  [27], and for 100 realizations of disorder and two different values of the disorder amplitude  $\Delta$ . For normal

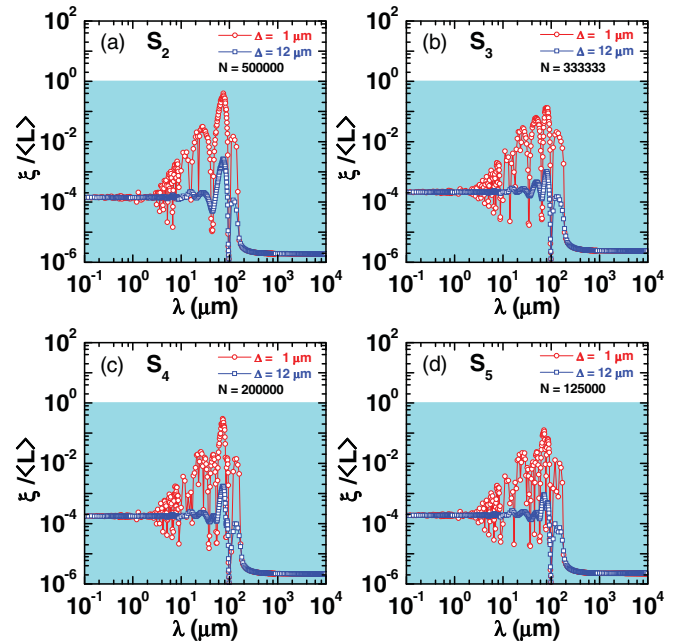


FIG. 7. (Color online) As described in the legend of Fig. 5, but for the magnetic permeability given by Eq. (10) with  $\mu_0 = 1$ ,  $F = 0.25$ ,  $\omega_m = 6\pi$  THz, and  $\gamma_m = 0$ . Other parameters were taken as described in the legend of Fig. 5.

incidence, the localization length does not display a power-of- $\lambda$  dependence in the limit  $\lambda \rightarrow \infty$  and, for any value of  $\lambda$ , there is no suppression of Anderson localization. Present theoretical results indicate that the asymptotic behavior of  $\xi$  in the long wavelength region strongly depends on the kind of magnetic response of the metamaterial slabs. Of course, further theoretical work is required in the case of different values of the incidence angle and cases of more complicated metamaterials, with different dielectric and magnetic responses.

#### IV. CONCLUSIONS

Summing up, we have carried out an extensive investigation of the quasiperiodicity and structural disorder effects on the Brewster anomalies in disordered quasiperiodic photonic crystals. Numerical results indicate that the positions of the Brewster anomalies in the frequency spectra are independent of the system geometry, and are only determined by the incidence angle and dielectric and magnetic responses of the individual slabs composing the heterostructure. If Drude-like responses for both the dielectric permittivity and magnetic permeability of the metamaterial slabs are chosen, we have also shown that quasiperiodicity may affect the behavior of the

localization length ( $\xi$ ) as a function of the vacuum wavelength mainly in the long-wavelength regime where  $\xi$  increases as a power of  $\lambda$ . For normal incidence, some values of the power of  $\lambda$  were computed from its corresponding numerical data via a statistical analysis, and obtained results display a slight discrepancy with the  $\gamma = 6$  value predicted by Asatryan *et al.* [6]. Moreover, we have demonstrated that, by replacing the Drude-like magnetic permeability by a more realistic one in the long wavelength limit, the asymptotic behavior of the localization length may be dramatically modified. Therefore, the present study suggests that the asymptotic behavior of the localization length in the long wavelength region may be strongly influenced by the kind of dielectric and magnetic responses of the individual layers. Finally, we do hope the present work will contribute to stimulate further theoretical and experimental research in this area.

#### ACKNOWLEDGMENTS

E.R.-G. and A.B.-A. thank the Instituto de Física, UNICAMP, Brazil, where part of this work was performed. The present work was partially financed by the Brazilian Agencies CNPq and FAPESP as well as the Scientific Colombian Agency CODI-University of Antioquia.

- 
- [1] Lord Rayleigh, *Phil. Mag.* **S.5** **24**, 145 (1887).
  - [2] V. G. Veselago, *Sov. Phys. Usp.* **10**, 509 (1968).
  - [3] E. Reyes-Gómez, D. Mogilevtsev, S. B. Cavalcanti, C. A. A. de Carvalho, and L. E. Oliveira, *Europhys. Lett.* **88**, 24002 (2009).
  - [4] C. A. A. de Carvalho, S. B. Cavalcanti, E. Reyes-Gómez, and L. E. Oliveira, *Phys. Rev. B* **83**, 081408(R) (2011).
  - [5] C. Fu, Z. M. Zhang, and P. N. First, *Appl. Opt.* **44**, 3716 (2005).
  - [6] A. A. Asatryan, L. C. Botten, M. A. Byrne, V. D. Freilikher, S. A. Gredeskul, I. V. Shadrivov, R. C. McPhedran, and Y. S. Kivshar, *Phys. Rev. Lett.* **99**, 193902 (2007).
  - [7] F. M. Izrailev and N. M. Makarov, *Phys. Rev. Lett.* **102**, 203901 (2009).
  - [8] D. Mogilevtsev, F. A. Pinheiro, R. R. dos Santos, S. B. Cavalcanti, and L. E. Oliveira, *Phys. Rev. B* **82**, 081105(R) (2010).
  - [9] A. Bruno-Alfonso, E. Reyes-Gómez, S. B. Cavalcanti, and L. E. Oliveira, *Phys. Rev. A* **78**, 035801 (2008).
  - [10] E. Reyes-Gómez, N. Raigoza, S. B. Cavalcanti, C. A. A. de Carvalho, and L. E. Oliveira, *Phys. Rev. B* **81**, 153101 (2010).
  - [11] E. Reyes-Gómez, N. Raigoza, S. B. Cavalcanti, C. A. A. de Carvalho, and L. E. Oliveira, *J. Phys. Condens. Matter* **22**, 385901 (2010).
  - [12] D. R. Smith, J. B. Pendry, and M. C. K. Wiltshire, *Science* **305**, 788 (2004).
  - [13] A. G. Aronov and V. M. Gasparian, *Solid State Commun.* **73**, 61 (1990).
  - [14] A. G. Aronov, V. M. Gasparian, and U. Gummich, *J. Phys. Condens. Matter* **3**, 3023 (1991).
  - [15] J. B. Pendry, *Advances Physics* **43**, 461 (1994).
  - [16] M. M. Sigalas, C. M. Soukoulis, C. T. Chan, R. Biswas, and K. M. Ho, *Phys. Rev. B* **59**, 12767 (1999).
  - [17] J. Bertolotti, S. Gottardo, D. S. Wiersma, M. Ghulinyan, and L. Pavesi, *Phys. Rev. Lett.* **94**, 113903 (2005).
  - [18] J. Bertolotti, M. Galli, R. Sapienza, M. Ghulinyan, S. Gottardo, L. C. Andreani, L. Pavesi, and D. S. Wiersma, *Phys. Rev. E* **74**, 035602 (2006).
  - [19] S. F. Liew and H. Cao, *J. Opt.* **12**, 024011 (2010).
  - [20] A. R. McGurn, K. T. Christensen, F. M. Mueller, and A. A. Maradudin, *Phys. Rev. B* **47**, 13120 (1993).
  - [21] D. S. Wiersma, P. Bartolini, A. Lagendijk, and R. Righini, *Nature (London)* **390**, 671 (1997).
  - [22] J. Topolancik, B. Ilic, and F. Vollmer, *Phys. Rev. Lett.* **99**, 253901 (2007).
  - [23] Y. Lahini, A. Avidan, F. Pozzi, M. Sorel, R. Morandotti, D. N. Christodoulides, and Y. Silberberg, *Phys. Rev. Lett.* **100**, 013906 (2008).
  - [24] S. A. Ramakrishna, *Rep. Prog. Phys.* **68**, 449 (2005).
  - [25] P. Sheng, *Introduction to Wave Scattering, Localization, and Mesoscopic Phenomena* (Academic, New York, 1995).
  - [26] T. J. Yen, W. J. Padilla, N. Fang, D. C. Vier, D. R. Smith, J. B. Pendry, D. N. Basov, and X. Zhang, *Science* **303**, 1494 (2004).
  - [27] F. S. S. Rosa, D. A. R. Dalvit, and P. W. Milonni, *Phys. Rev. Lett.* **100**, 183602 (2008).
  - [28] R. S. Penciu, M. Kafesaki, Th. Koschny, E. N. Economou, and C. M. Soukoulis, *Phys. Rev. B* **81**, 235111 (2010).